http://dx.doi.org/10.5455/sf.99872

Science Forum (Journal of Pure and Applied Sciences)

journal homepage: www.atbuscienceforum.com

Amperometric immunosensor based on the conducting layer of PAni/Fe_3O_4 nanocomposites for the detection of $A\beta_{42}$

Auwal Adamu Mahmoud[1*], Mohd Kamarulzaki Mustafa[2], Nurun Najwa Ruslan[2], Aliyu Jauro[1], Ibrahim Hassan Garba[3], Umar Farouk Hassan[1]

[1] *Department of Chemistry, Faculty of Science, Abubakar Tafawa Balewa University, Bauchi, Nigeria*

[2] *Faculty of Science and Applied Technology, Universiti Tun Hussein Onn Malaysia, Parit Raja, Johor. Malaysia*

[3] *Department of Biochemistry, Faculty of Science, Abubakar Tafawa Balewa University, Bauchi, Nigeria*

ABSTRACT

Conducting PAni/Fe_3O_4 nanocomposites were synthesized and electrochemically deposited on fluorine-tin-oxide (FTO)-coated glass to form a transducing layer owing to their catalytic, magnetic, and electrical properties. This synthesized conducting layer was used to immobilized anti-β_{42} for the detection of Alzheimer's disease. The electrode modification process was characterized by electrochemical impedance spectroscopy, cyclic voltammetry, and field emission scanning electron microscopy. Some factors influencing the performance of the amperometric immunosensor were optimized. The experiment outcome indicates a conducting layer of the nanocomposites on the FTO-coated glass in the range of −1.5 to 0.5 V at 0.10 Vs^{-1} in a 10 ml solution of PAni-Fe_3O_4 nanocomposites. Electrochemical impedance changes occurred only after PAni/Fe_3O_4 bound to surface of bare FTO, confirming the deposition and indicating that the new modified electrode can be used as a transducing matrix for the immobilization of the biomarker. Tests performed with this immunosensor showed good linearity with a detection limit of 0.061 $\mu g/ml^{-1}$ at 3σ.

ARTICLE INFO

Article history:
Received 09 March 2022
Received in revised form
13 March 2022
Accepted 14 March 2022
Published 27 April 2022
Available online 27 April 2022

KEYWORDS

Immunosensor
Polyaniline
Nanocomposites
Conductivity
Fe_3O_4
β-amyloid

1. Introduction

Conducting polymers have recently been considered as suitable matrices for immobilization of biomolecules (Dhand et al., 2007). This has been attributed to a number of factors, such as flexibility in chemical structure required for binding with biomolecules (Basniwal et al., 2013), efficient signal transduction, and unique electron transfer capabilities (Haldorai et al., 2011). They are also capable of penetrating the insulating the shell of biomolecules and providing a means for direct electrical communication between the redox center and the electrode surface (Dhand et al., 2011).

There is also a growing interest on polyaniline nanostructured material for the fabrication of biosensor interfaces. PAni is ideally suited for the covalent binding of biomolecules (DNA and enzymes) due to the available active functional groups (Dhand et al., 2010b). Furthermore, the properties of PAni, such as its shape and dimensions, can be fine-tuned and controlled during the synthesis (Ding et al., 2007) by varying synthesis parameters or processing conditions which normally result in desired physical and electrochemical properties for biosensing applications.

* **Corresponding author** A. A. Mahmoud ✉ aamahmoud@atbu.edu.ng ✉ Department of Chemistry, Faculty of Science, Abubakar Tafawa Balewa University, Bauchi, Nigeria.

An early sensitive detection of the β-amyloid level in the blood is very important for proper treatment to reduce the risk of Alzheimer's disease (Shaw et al., 2009). The fabrication of immunosensors based on antigen/antibody complex formation for analytical purposes have been successfully applied to many fields, including environmental protection (Mauriz et al., 2007), food analysis (Duran and Marcato, 2013), and clinical diagnosis (Tang et al., 2008; Zhong et al., 2010). An effective combination of antibody–antigen specificity in a biosensor device with a transducer could lead to the basis of direct detection of several ranges of analytes with high sensitivity and selectivity. This analytical device works based on changes in heat, mass, electrochemical, or optical properties.

Electrochemical methods have drawn more attention than other transduction methods (Martín-Yerga et al., 2012) and have a wide range of uses due to their simple pretreatment procedure (Lucarelli et al., 2008), fast analytical time, precise and sensitive current measurement, and inexpensive and miniaturizable instrumentation (Zang et al., 2012). In electrochemical immunosensors, the amount of analyte is determine by detecting the changes of conductance, current, potential, or impedance caused by the immunoreaction (Ronkainen et al., 2010). In these methods, the amperometric immunosensor is especially promising because of its simplicity, high sensitivity, and relatively low detection limit (Chang and Park, 2010).

In order to obtain high sensitivity and good selectivity of the immunosensor, suitably functional electrode materials should be developed in the fabrication of electrochemical sensing. Various materials have been used for the preparation of the conducting layer of the electrode, among which are metal nanoparticles (Zhang et al., 2012), conductive polymers (Turkmen et al., 2014), metal oxides, and carbon materials (He et al., 2015).

2. Experimental Study

2.1. Materials and methods

Aniline monomer (99.9%) was supplied by R&M chemicals and distilled under reduced pressure before storage at a temperature below 0°C. All other chemicals and reagents were of analytical grade and were used without additional purification: ammonium peroxydisulfate (APS), phosphoric acid (H_3PO_4), N-phenyl-1,4-phenylenediamine, acetonitrile, CH_2Cl_2, formic acid, $FeCl_2{\cdot}4H_2O$, $FeCl_3{\cdot}6H_2O$, diethyl ether, and $NH_3{\cdot}H_2O$ (25%). Succinic anhydride, methanol, ammonium hydroxide, and glutaraldehyde were supplied by QReC. β-amyloid, anti-β-amyloid, and 0.1% bovine serum albumin (BSA) were supplied by Sigma-Aldrich and were prepared in a phosphate buffer (50 mM, pH 7.0). Phosphate buffer solution (PBS), pH 7.0, was used as a redox mediator and solvent for making various antigen concentrations; 10 mM $K_3[Fe(CN)_6]$+$K_4[Fe(CN)_6]$ was used as the redox probe during electrochemical measurements and was also supplied by QReC.

2.2. Preparation of PAni-Fe_3O_4 composites

The technique reported previously (Adamu et al., 2015; Lu et al., 2005) was used to synthesize Fe_3O_4 nanoparticles, while PAni-Fe_3O_4 nanocomposites were synthesized by the ultrasonic irradiation method. In a typical procedure, 0.2 mL aniline monomer was mixed with H_3PO_4 (0.07 ml) and different wt% of Fe_3O_4 dissolved in 15 ml of deionized water under ultrasonic irradiation for 10 minutes to disperse Fe_3O_4 nanoparticles and to form a mixture of the aniline/H_3PO_4 complex containing Fe_3O_4 nanoparticles. Then, 0.46 g of APS was added to the mixture. The reaction was kept by ultrasonic mixing for 4 hours between 25°C and 30°C. The suspension turned green immediately after the addition of APS indicating the polymerization of aniline. The resulting precipitate (blackish green) was obtained by filtering and washing the reaction mixture with distilled water and ethanol, respectively. Finally, the nanocomposites were vacuum dried in at 70°C for 24 hours.

2.3. Electrode modification

The fabrication of PAni/Fe_3O_4/fluorine-tin-oxide (FTO) was carried out using cyclic voltammetry. An FTO-coated glass plate with an area dimension of 1.27 × 2.54 × 0.1 cm^2 and a resistance value ranging from 17 to 28 ohm was used. The FTO-coated glass was sonicated in acetone, ethanol, and distilled water for 10 min consequently. The clean FTO substrate was then immersed in 1:7 v/v ammonium hydroxide solution for 1 hour to attach the hydroxyl groups on the FTO surface.

2.4. Fabrication of the transducing layer

The electrochemical deposition of the nanocomposites on the FTO was carried out by cyclic voltammetry in typical conventional electrochemical cells containing 10 ml of colloidal suspension of PAni/Fe_3O_4 nanocomposites prepared by forming a solution of PAni-Fe_3O_4/formic acid (1 mg ml^{-1}) in 9.9 ml of acetonitrile at room temperature in a three-electrode setup where bare unmodified FTO-coated glass was used as the working electrode (deposition substrate). A platinum wire and Ag/AgCl as counter and reference electrodes, respectively, were dipped into the colloidal solution and the PAni/Fe_3O_4 were electrodeposited at

an applied voltage of +1.5 V for 10 min on the surface of the FTO-coated glass. The cyclic voltammetry (CV) with the potential swept from −0.3 to 0.3 (*vs.* Ag/AgCl) and a scan rate of 0.1 V/s was used for the interrogation of the electrode at different modification stages.

2.5. Electrochemical impedance spectroscopy (EIS) analysis

EIS was utilized to monitor analyte recognition using Nova 1.10 software. The impedance measurements of the electrodes were performed within a range of frequencies from 0.1 Hz to 10,000 Hz at 220 mV versus Ag/AgCl. EIS reading was recorded before and after deposition of the PAni/Fe_3O_4 nanocomposites, and also after antibody immobilization.

2.6. Characterization

The surface morphology of the modification process was examined from field emission scanning electron microscope (FESEM, JEOL, JSM-7600F). The fabricated electrodes PAni/Fe_3O_4/FTO and anti-β-amyloid/PAni/Fe_3O_4/FTO were characterized using PerkinElmer's Fourier transform infrared (FT-IR) spectrometer (Model spectrum 100 with ATR sampling accessory). The LUCAS LABS Pro4 was used to measure the electron transport behavior of the nanocomposites and the modified electrode. The dried PAni/Fe_3O_4 nanocomposite powders were pelletized by hydraulic press (10 MPa for 5 minutes). DC resistance of pellets was measured and from the measured resistance and the sample dimensions, the conductivity value was calculated. The Park System's atomic force microscopy (AFM) XE-100 was used to investigate the morphology and microstructure of the nanocomposites and the modified electrode in a noncontact mode.

3. Results and Discussion

3.1. Morphological characteristics of the resulting different surfaces of the modified electrode during each step of the fabrication process

FESEM was used to characterize the surface morphologies of the modified electrode layers at different stages of fabrication. Bare FTO substrate showed a very rough but homogeneous surface (Fig. 1a), whereas PAni/Fe_3O_4/FTO showed the nanotube lying next to each other, as well as on the electrode surface (Fig. 1c). The nanocomposites were dispersed on the substrate during the deposition process. This proved the successful deposition of PAni/Fe_3O_4 nanocomposites on the FTO-coated glass (Fig. 1c); however, after immobilization of anti-β-amyloid on the modified electrode, it showed that the distributed nanotube covered with sticky paste-like material possibly arising from the interaction between PAni/Fe_3O_4 nanocomposites and the antibody and the aggregation

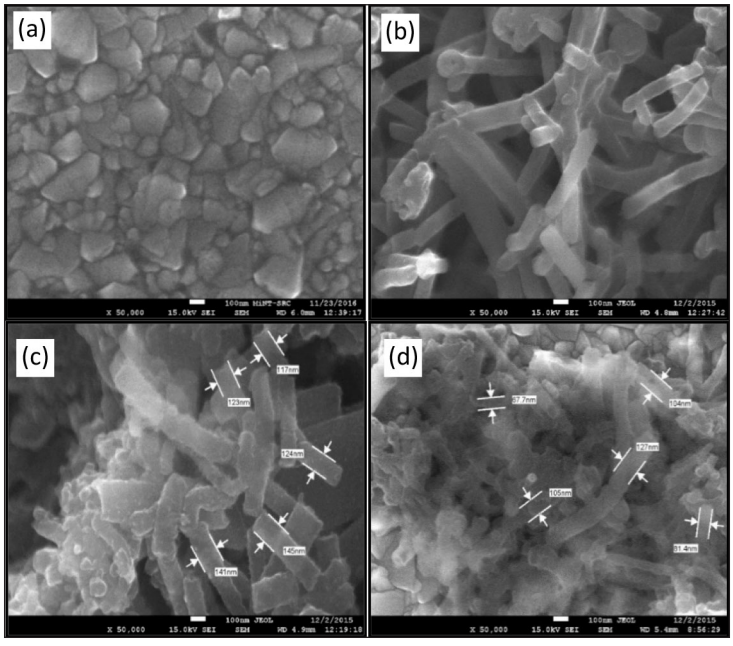

Figure 1. FESEM characterization of the modified electrode surfaces. (a) Bare FTO, (b) PAni/Fe_3O_4 nanocomposites, (c) PAni/Fe_3O_4/FTO-modified electrode, and (d) anti-β-amyloid/PAni/Fe_3O_4/FTO bioelectrode.

of anti-β-amyloid molecule during immobilization (Fig. 1d). The FTO-coated glass surface is clearly seen in the background (Fig. 1c and d).

These results suggest the presence of antibodies on the electrode. The use of glutaraldehyde for covalent immobilization of antibodies has further resulted in the direct binding of anti-β-amyloid with PAni/Fe_3O_4 nanocomposites and is expected to prevent the leaching problem that might cause reduction in the sensing response during extended measurements (Dhand et al., 2010a). Eventually, the results of the morphological study were in good agreement with those obtained from impedance characterization studies.

3.2. FT-IR Spectra of PAni/Fe_3O_4/FTO-modified electrode and anti-β-amyloid/PAni/Fe_3O_4/FTO bioelectrode

Figure 2(c) shows the FT-IR spectra of PAni/Fe_3O_4/FTO revealing absorption bands at 1,568 and 1,487 cm^{-1} (corresponding to the C = C stretching deformation of quinoid and benzenoid rings), 1,291 cm^{-1} (attributed to the C–N stretching of secondary aromatic amine), 1,237 cm^{-1} (assigned to the aromatic C–H in-plane bending), and 798 cm^{-1} (related to out-of-plane deformation of C–H in the 1,4-disubstituted benzene ring). The band seen at 691 cm^{-1} may be ascribed to the absorption of -PO_4 group revealing doping of polyaniline with the phosphoric acid (H_3PO_4).

The FT-IR spectrum of anti-Aβ_{42}/PAni/Fe_3O_4/FTO bioelectrode, as shown in Figure 2(d), exhibits additional absorption bands at 1,991 cm^{-1} (carbonyl stretch, amide I band), whereas the peak at 3,213 cm^{-1} originated from N–H stretching (amide A) and 2,113 cm^{-1} from N–H stretching (amide B), revealing the successful immobilization of anti-Aβ_{42} on the modified PAni/Fe_3O_4/FTO electrode surface.

3.3. Surface roughness studies

AFM studies have also been carried out on the bare and modified electrodes. The 3D micrograph of the nanocomposite film (Fig. 3b) reveals a homogeneous rough surface morphology of PAni/Fe_3O_4 on the FTO-coated glass. The value of the roughness (estimated as root mean square, rms) of the modified electrode obtained using height distribution analysis has been found to be 30.50 nm. It may be noted that this value of the roughness is higher than that of the bare FTO-coated glass (27.49 nm) (Fig. 3a and b), which indicates increased available surface.

However, after the immobilization of the antibodies (Fig. 3c) and immunoreaction (Fig. 3d), the roughness increases and the surface becomes less homogeneous. The progressive increase in the value of rms is an indication confirming the antibody binding and the subsequent immunoreaction on the modified electrode surface. This finding is in consistence with that of Karir et al. (2006), who found out that the AFM analysis shows enhanced roughness in the case of PAni-modified surfaces as compared to the unmodified one, allowing more adsorption of antibodies to the surface (Karir et al., 2006). Eventually, the results obtained with FESEM and AFM were also in good agreement with those obtained from impedance characterization studies.

3.4. Electrical conductivity of the PAni/Fe_3O_4 nanocomposites and the modified electrode PAni/Fe_3O_4/FTO

Using the cyclic voltammetry technique, the layers of PAni/Fe_3O_4 nanocomposite are formed on the FTO glass surface at an applied voltage of +1.5 V for 10–40 minutes. In order to confirm the successful deposition

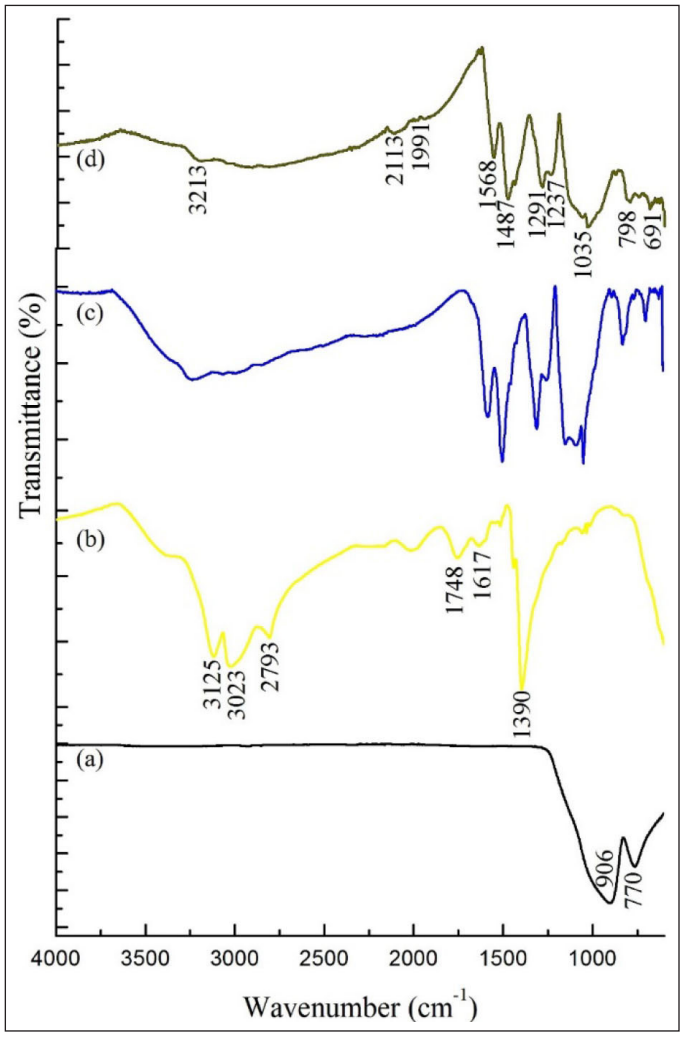

Figure 2. FT-IR spectra of (a) Bare FTO, (b) Fe_3O_4, (c) PAni/Fe_3O_4/FTO, and (d) anti-β-amyloid/PAni/Fe_3O_4/FTO.

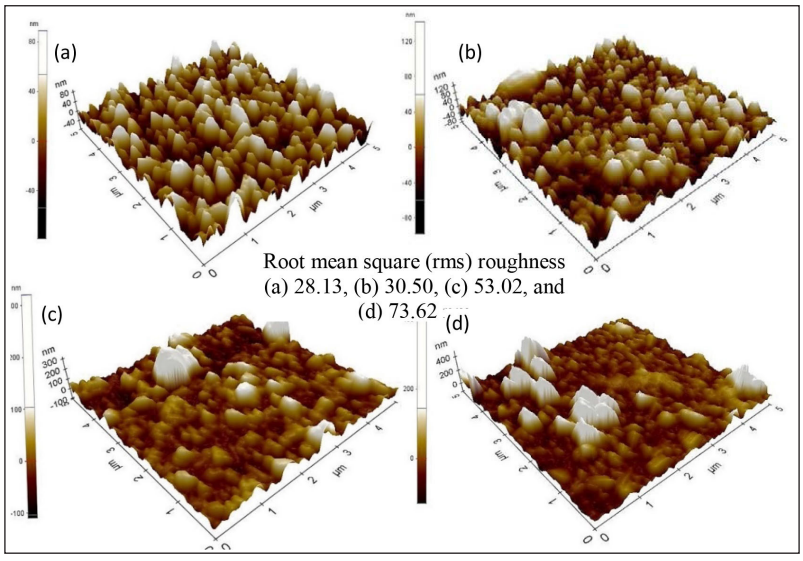

Figure 3. AFM images of (a) bare FTO, (b) modified PAni/Fe_3O_4/FTO electrode, (c) anti-$A\beta_{42}$/PAni/Fe_3O_4/FTO, and (d) $A\beta_{42}$/anti-$A\beta_{42}$/PAni/Fe_3O_4/FTO.

of the nanocomposites on the FTO-coated glass, the room temperature conductivity of the modified electrode PAni/Fe_3O_4/FTO was measured at different deposition times (see Fig. 3a).

The conductivity of the modified electrode increases with deposition time possibly due to grain to grain electrodeposition of the nanocomposites (Haldorai et al., 2011). The conductivity reaches its optimum value of 1.482 $\times 10^{-3}$S/cm after 30 minutes of deposition (Fig. 4a). This result indicates the successful formation of a conductive layer for the electrochemical transduction.

The influence of the degree of protonation also affects the room temperature conductivity of the nanocomposites during the synthesis of the nanocomposites (as can be seen in Fig. 4b). An increase in conductivity with an increase in the amount of dopant results in the increase of conductivity with an increase in the amount of H_3PO_4, as reported earlier (Adamu et al., 2015).

The nanocomposites with the highest conductivity were used as the conductive layer of the modified electrode. It is interesting to know that PAni/Fe_3O_4 nanocomposites after retaining some of its unique properties, like flexibility, ease of processing and synthesis, are now having good electrical conductivity.

3.4.1. Electrochemical properties of the layer by layer assembly of the immunosensor

Figure 5 shows a typical Nyquist diagram of the impedance spectra of the stepwise assembly of the immunosensor in the presence of the redox probe, 10 mM $K_3Fe(CN)_6$ + $K_4Fe(CN)_6$ (1:1 ratio) and 10 Mm PBS, pH 7.0, at 25°C.

In Nyquist plots, the complex impedance is displayed as the sum of the real and imaginary components (Z_{real} and Z_{imag}, respectively); the semicircle diameter at higher frequencies corresponds to the electron transfer resistance (R_{et}); and the linear part at lower frequencies corresponds to the diffusion process (Warburg impedance). The diameter of the semicircle also exhibits the blocking behavior of the modified electrode after each modification step. It can be seen that the bare FTO-coated glass exhibits an almost straight line (Fig. 5a), which was characteristic of a diffusional limiting step of the electrochemical process.

It is obvious that changes in electrochemical impedance occurred during the electrode modification step, i.e., after PAni/Fe_3O_4 bound to surface of bare FTO to form the thin conducting layer of PAni/Fe_3O_4 nanocomposites. During the deposition of PAni/Fe_3O_4 on FTO-coated glass, the impedance spectra showed a facilitated electron transfer on the electrode surface. The charge transfer resistance (R_{ct}) values decreased significantly after the nanocomposites formation on the FTO-coated glass owing to formation of amino ends, which might help the redox probe to diffuse onto the electrode surface (Fig. 5b).

However, immobilization of anti-β-amyloid on the modified electrode PAni/Fe_3O_4/FTO via glutaraldehyde showed a remarkable increase in the electron transfer resistance R_{ct} values. In this case, anti-β-amyloid

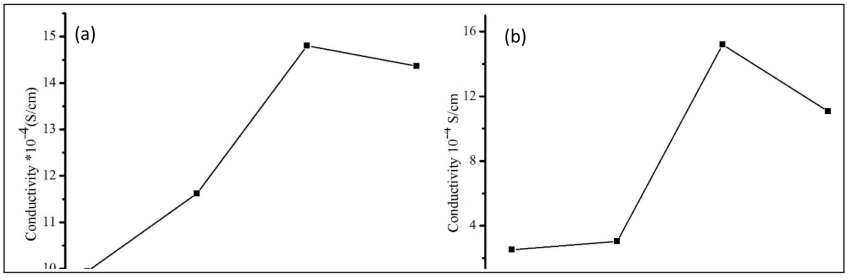

Figure 4. Room temperature conductivity of (a) the nanocomposites at different amounts of H_3PO_4 and (b) the modified electrode PAni/Fe_3O_4/FTO at different deposition times

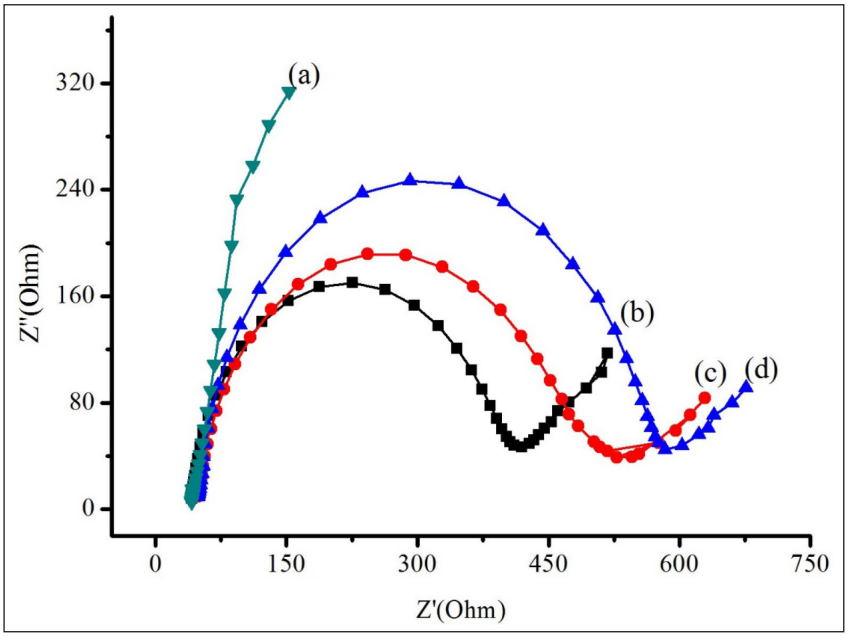

Figure 5. Electrochemical impedance of (a) bare FTO, (b) PAni/Fe3O4/FTO-modified electrode, (c) anti-β-amyloid/PAni/Fe3O4/FTO bioelectrode, and (d) β-amyloid/anti-β-amyloid/PAni/Fe3O4/FTO measured in 10 mM [Fe(CN)6]3-/4- solution.

probably exhibited higher resistances against the diffusion of redox probe molecules (Fig. 5c). This can be attributed to the insulating nature of anti-β-amyloids that inhibit the permeability of $[Fe(CN)_6]^{3-/4-}$ to the electrode surface and also indicates the presence of anti-β-amyloids on the modified electrode, which blocks the electron exchange between the redox probe and the electrode surface (Fig. 5c).

The interaction between anti-β-amyloid and β-amyloid made the electron resistance increase further (Fig. 5d). After the immunoreactions, the β-amyloid was captured on the immunosensor surface by the anti-β-amyloid; the semicircle increased distinctively, indicating that the particular interaction hindered the electron transfer between the electrochemical probe $[Fe(CN)_6]^{3-/4-}$ and the electrode (Fig. 5d).The increase in electron transfer resistance with immobilization of antibodies on the glass substrate was also reported by Canbaz and Sezgintürk (2014). These results also suggest a successful immunoreaction between the anti-β-amyloid and β-amyloid. It can be concluded here that a good linear relationship between semicircle diameters and electrode layers indicates successful construction of the immunosensor.

3.5. Cyclic Voltammograms of the electrodes at different stages of modification

The assembly process of β-amyloid/anti-β-amyloid/PAni/Fe_3O_4/FTO multilayer films on the FTO glass was monitored by CV experiments. From Figure 6, it is evident that the redox label $[Fe(CN)_6]^{3-/4-}$ reveals a stable and well-defined reversible cyclic voltammogram

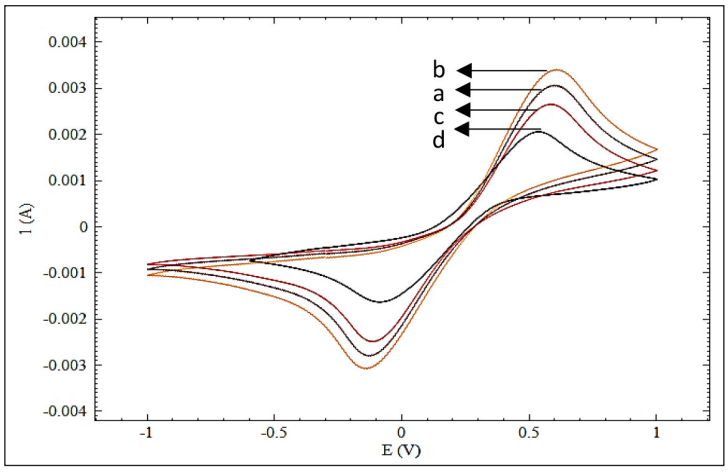

Figure 6. Cyclic voltammogram of the modified electrode measured in 10 mM $[Fe(CN)_6]^{3-/4-}$ (1:1 ratio) in 10 mM PBS, pH 7.0. (a) Bare FTO, (b) PAni/Fe_3O_4/FTO, (c) anti-β-amyloid/PAni/Fe_3O_4/FTO, and (d) β-amyloid/anti-β-amyloid/PAni/Fe_3O_4/FTO.

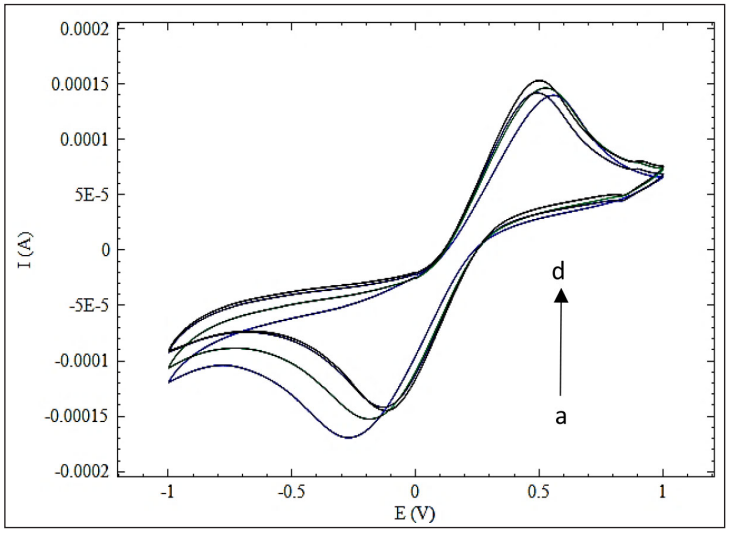

Figure 7. Cyclic voltammograms of the immunosensor in 10 mM [Fe(CN)6]3-/4- (1:1 ratio) in 10 mM PBS, pH 7.0, at a scan rate of (a) 0.02, (b) 0.05, (c) 0.1, and (d) 0.15 V/s, respectively (from the inner to outer).

on the bare FTO-coated glass electrode (curve a). However, after the electrodeposition of the PAni/Fe_3O_4 nanocomposites on the FTO-coated glass electrode, there is a good redox performance, with an obvious increase in the peak current (curve b); this can be attributed to the amplification effects of the conducting PAni/Fe_3O_4 nanocomposites and similar to the EIS results, it could indicate facilitated electron transfer between the nanocomposites and the FTO surface.

The decrease in the redox peak currents was observed after the immobilization of anti-β-amyloid on the surface of the modified electrode (curve c), suggesting a reduction in the electron flow because the membrane is becoming less conductive due to the insulating property of the antibodies, an indication that anti-β-amyloid has been immobilized on the electrode surface. A much higher drop in peak is observed after incubating the immunosensor with 0.01 μg mL^{-1} β-amyloid (curve d). The antibody/antigen reaction forms a β-amyloid/anti-β-amyloid immunocomplex which acts as the inert electron and mass transfer blocking layer hindering the transfer of the electron toward the surface of the electrode. These results were in agreement with that of the FESEM, FTIR, and EIS,

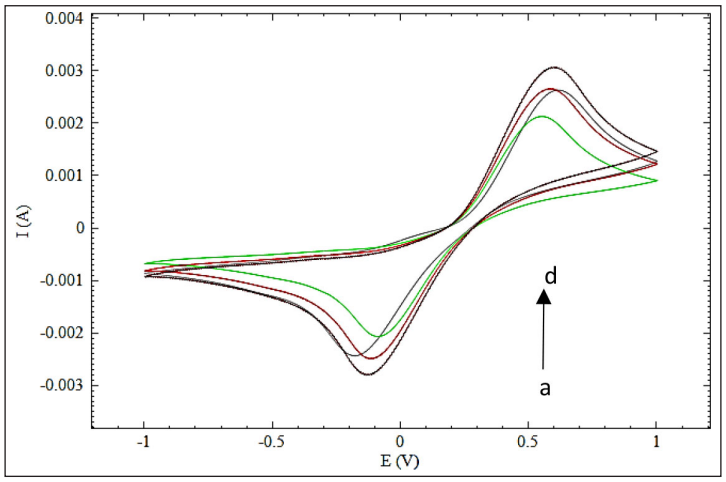

Figure 8. Cyclic voltammogram of anti-β-amyloid immobilized electrode with different concentrations of the β-amyloid. (a) 0.00001. (b) 0.0001. (c) 0.001. (d) 0.01 μgmL^{-1}.

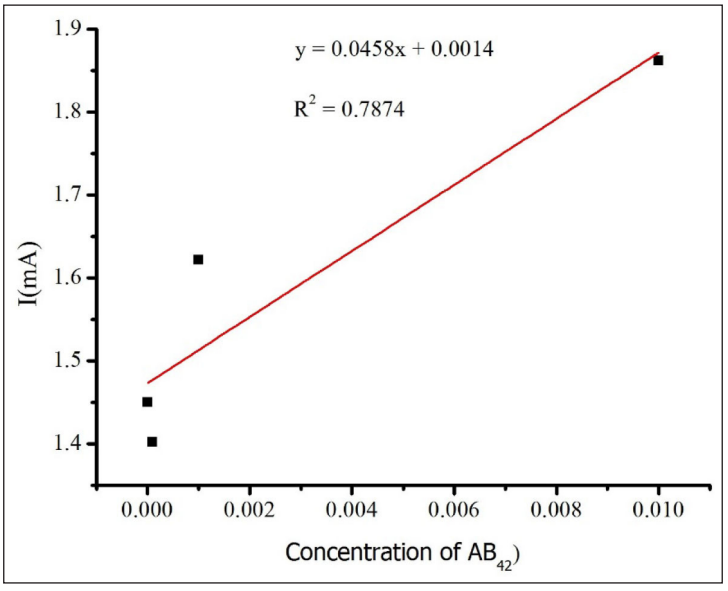

Figure 9. The effect of β-amyloid concentration (μg ml^{-1}) upon the amperometric response of the immunosensor.

and demonstrated the stepwise modifying process of the electrode.

The cyclic voltammograms of the resulting immunosensor in 10 mM $[Fe(CN)_6]^{3-/4-}$(1:1 ratio) in 10 mM PBS, pH 7.0, at different scan rates were investigated. With the increase in scan rate, the peak currents also increased. Square root of the scan rate from 0.02 to 0.15 V/s showed a linear relationship with peak current, indicating a diffusion controlled behavior (Shi et al., 2007).

3.6. Detection of β-amyloid

Figure 8 shows the CVs of the anti-β-amyloid/PAni/Fe_3O_4/FTO modified bioelectrode with different concentrations of β-amyloid. The cathodic peak current responses of CVs were plotted and were found to be proportional to the concentration of β-amyloid in the range from 0.0001 to 0.01 μg ml^{-1}.

The linear regression equation was determined and is given as follows:

$$y = 0.0458x + 0.0014 \quad (1)$$

with a correlation coefficient of 0.7874 (Fig. 9).

The limit of detection (LOD; minimum detectable concentration of the analyte) for the immunosensor (anti-β-amyloid/PAni/Fe_3O_4/FTO) bioelectrode was also calculated from the linear regression analysis

result using Equation (2) and was found to be 0.061 μg ml^{-1} at 3σ.

$$\text{Limit of detection} = \frac{3 \times \text{SD}}{\text{Slop of the calibration curve}} \quad (2)$$

The stability of this bioelectrode is assigned to the high surface free energy provided by the PAni/Fe_3O_4 nanocomposites that help to strengthen the binding of biomolecules. Covalent immobilization of antibody using glutaraldehyde further results in direct binding of anti-β-amyloid with PAni/Fe_3O_4, preventing the leaching problem that may be responsible for decrease in the sensing response during prolonged measurements (Dhand et al., 2010).

3.7. Selectivity of the immunosensor

To investigate the specificity of the immunosensor, 0.01 μg ml^{-1} of hCG and 0.01 μg m^{-1} BSA were used for the incubation of the modified bioelectrode. It is interesting to find that no remarkable difference of peak currents was obtained as compared to 0.01 μg ml^{-1} β-amyloid. Thus, it can be concluded that the immunosensor had a good selectivity to β-amyloid and therefore the immunosensor can serve an appropriate tool for the detection of β-amyloid.

4. Conclusion

The Alzheimer's disease immunosensor was also successfully fabricated based on the synthesized PAni/Fe_3O_4 films deposited electrochemically onto FTO-coated glass substrates. Anti-β-amyloid has been covalently immobilized onto the modified electrode films. The detection limit is calculated after measuring the current response of the immunosensor with different concentrations of β-amyloid. The cathodic peak current responses of CVs were plotted and were found to be proportional to the concentration of β-amyloid in the range of 0.00001–0.01 μg ml^{-1}.

The linear regression equation was I = 0.0458Cβ-amyloid + 0.0014; and correlation coefficient was 0.7874. The LOD was found to be 0.061 μg ml^{-1} at 3σ.

The stability of this bioelectrode is assigned to the high surface free energy provided by the PAni/Fe_3O_4 nanocomposites that help to strengthen the binding of biomolecule. Covalent immobilization of antibody using glutaraldehyde further results in direct binding of anti-β-amyloid with PAni/Fe_3O_4, preventing the leaching problem that may be responsible for the decrease in the sensing response during prolonged measurements (Dhand et al., 2010).

This study also shows the possibility of using PAni/Fe_3O_4/FTO electrode as a new biosensor platform for the immobilization of other antibodies for immunosensing. Further study will be dedicated to analyzing the sensitivity, specificity, and stability of the biosensor to detect β-amyloid in serum samples. Similar studies should be conducted using other biomarkers.

References

Adamu MA, Mustafa MK, Ruslan NN. Mophology of polyaniline nanotube with various level of Fe3O4 nanoparticles and their electrical conductivities by ultrasonic dispersion method. J Eng Appl Sci 2015; 11(16):9725–9.

Basniwal RK, Chauhan RPS, Parvez S, Jain VK. Development of a cholesterol biosensor by chronoamperometric deposition of polyaniline-Ag nanocomposites. Int J Polymeric Mater Polymeric Biomater 2013; 62(9):493–8.

Canbaz MÇ, Sezgintürk MK. Fabrication of a highly sensitive disposable immunosensor based on indium tin oxide substrates for cancer biomarker detection. Anal Biochem 2014; 446:9–18.

Chang B-Y, Park S-M. Electrochemical impedance spectroscopy. Ann Rev Anal Chem 2010; 3:207–29.

Dhand C, Das M, Datta M, Malhotra B. Recent advances in polyaniline based biosensors. Biosens Bioelectron 2011; 26(6):2811–21.

Dhand C, Das M, Sumana G, Srivastava AK, Pandey MK, Kim CG, et al. Preparation, characterization and application of polyaniline nanospheres to biosensing. Nanoscale, 2010a; 2(5):747–54.

Dhand C, Singh S, Arya SK, Datta M, Malhotra B. Cholesterol biosensor based on electrophoretically deposited conducting polymer film derived from nano-structured polyaniline colloidal suspension. Anal Chim Acta 2007; 602(2):244–51.

Dhand C, Sumana G, Datta M, Malhotra B. Electrophoretically deposited nano-structured polyaniline film for glucose sensing. Thin Solid Films 2010b; 519(3):1145–50.

Ding H, Wan M, Wei Y. Controlling the diameter of polyaniline nanofibers by adjusting the oxidant redox potential. Adv Mater 2007; 19(3):465–9.

Duran N, Marcato PD. Nanobiotechnology perspectives. Role of nanotechnology in the food industry: a review. Int J Food Sci Technol 2013; 48(6):1127–34.

Haldorai Y, Nguyen VH, Pham QL, Shim J-J. Nanostructured materials with conducting and magnetic properties: preparation of magnetite/conducting copolymer hybrid nanocomposites by ultrasonic irradiation. Comp Interf 2011; 18(3):259–74.

He D, Zheng C, Wang Q, He C, Lee Y-I, Wu L, Hou X. Dielectric barrier discharge-assisted one-pot synthesis of carbon quantum dots as fluorescent probes for selective and sensitive detection of hydrogen peroxide and glucose. Talanta 2015; 142:51–6.

Karir T, Hassan P, Kulshreshtha S, Samuel G, Sivaprasad N, Meera V. Surface modification of polystyrene using polyaniline nanostructures for biomolecule adhesion in radioimmunoassays. Anal Chem 2006; 78(11):3577–82.

Lu X, Yu Y, Chen L, Mao H, Gao H, Wang J,et al. Aniline dimer–COOH assisted preparation of well-dispersed polyaniline–Fe3O4 nanoparticles. Nanotechnology 2005; 16(9):1660.

Lucarelli F, Tombelli S, Minunni M, Marrazza G, Mascini M. Electrochemical and piezoelectric DNA biosensors for hybridisation detection. Anal Chim Acta 2008; 609(2):139–59.

Martín-Yerga D, González-García MB, Costa-García A. Use of nanohybrid materials as electrochemical transducers for mercury sensors. Sensors Actuators B: Chem 2012; 165(1):143–50.

Mauriz E., Calle A, Manclus J, Montoya A, Lechuga LM. On-line determination of 3, 5, 6-trichloro-2-pyridinol in human urine samples by surface plasmon resonance immunosensing. Anal Bioanal Chem 2007; 387(8):2757–65.

Ronkainen NJ, Halsall HB, Heineman WR. Electrochemical biosensors. Chem Soc Rev 2010; 39(5):1747–63.

Shaw LM, Vanderstichele H, Knapik-Czajka M, Clark CM, Aisen PS, Petersen RC, et al. Cerebrospinal fluid biomarker signature in Alzheimer's disease neuroimaging initiative subjects. Ann Neurol 2009; 65(4):403–13.

Shi Y-T, Yuan R, Chai Y-Q, He X-L. Development of an amperometric immunosensor based on TiO 2 nanoparticles and gold nanoparticles. Electrochim Acta 2007; 52(11):3518–24.

Tang D, Yuan R, Chai Y. Ultrasensitive electrochemical immunosensor for clinical immunoassay using thionine-doped magnetic gold nanospheres as labels and horseradish peroxidase as enhancer. Anal Chem 2008; 80(5):1582–8.

Turkmen E, Bas SZ, Gulce H, Yildiz S. Glucose biosensor based on immobilization of glucose oxidase in electropolymerized poly (o-phenylenediamine) film on platinum nanoparticles-polyvinylferrocenium modified electrode. Electrochim Acta 2014; 123:93–102.

Zang D, Ge L, Yan M, Song X, Yu J. Electrochemical immunoassay on a 3D microfluidic paper-based device. Chem Commun 2012; 48(39):4683–5.

Zhang Y, Liu S, Wang L, Qin X., Tian, J., Lu, W., et al. One-pot green synthesis of Ag nanoparticles-graphene nanocomposites and their applications in SERS, H2O2, and glucose sensing. RSC Adv 2012; 2(2):538–45.

Zhong Z, Wu W, Wang D, Wang D, Shan J, Qing Y, et al. Nanogold-enwrapped graphene nanocomposites as trace labels for sensitivity enhancement of electrochemical immunosensors in clinical immunoassays: carcinoembryonic antigen as a model. Biosens Bioelectron 2010; 25(10):2379–83.